Benefits of Waveform Relaxation Method and Output Space Mapping for the Optimization of Multirate Systems

Antoine Pierquin, Stéphane Brisset, Thomas Henneron, Stéphane Clenet

Benefits of Waveform Relaxation Method and Output Space Mapping for the Optimization of Multirate Systems

A. Pierquin[1], S. Brisset[1], T. Henneron[2] and S. Clénet[3]

[1] EC Lille, L2EP,
Cité Scientifique - CS 20048 - 59651, Villeneuve d'Ascq, France.
e-mail: antoine.pierquin@ec-lille.fr
[2] Université de Lille, L2EP, Villeneuve d'Ascq, France
[3] Arts et Métiers ParisTech, L2EP, Lille, France

We present an optimization problem that requires to model a multirate system, composed of subsystems with different time constants. We use waveform relaxation method in order to simulate such a system. But computation time can be penalizing in an optimization context. Thus we apply output space mapping which uses several models of the system to accelerate optimization. Waveform relaxation method is one of the models used in output space mapping.

***Index Terms*—Differential algebraic equations, Electromagnetic coupling, Finite element methods, Optimization methods.**

I. Introduction

In the framework of the optimization of a multi-physics system, it is necessary to model the whole system and to perform a coupling of different numerical models. But modeling of a system including components with very different time constants is particularly problematic. On one hand, a strong coupling involves a time discretization according to the smallest time constant, and thus a large numerical system to solve and a long computation time. On the other hand, a weak coupling implies a lack of consistency of the results. In fact, a model used in optimization has to be as precise as possible but not too long to be computed because of the huge number of evaluations which the optimization process requires.

Waveform relaxation method (WRM) [1], [2] is an iterative process which allows to model each component of the multi-physics system with respect to its own time constant. This can reduce computation time, while keeping a good precision since the method converges to the exact solution [3], [4]. However, even WRM optimization can be extremely long to execute. With the aim of reducing more optimization time, an output space mapping (OSM) strategy [5], [6], [7], [8] can be set up. This is still an iterative process which requires at least two models of the same device, but with different accuracy and computation time. A coarse model, the fastest one, but the less accurate, is used during optimization. A fine model, the most time consuming, more precise, is evaluated once per iteration to correct the other model. Thus, the WRM can be used to produce the most precise model of the OSM.

The first two parts of this article present the waveform relaxation method and the output space mapping technique. In the last part, these methods are applied to the minimization of a transformer mass, using a finite element model (FEM).

II. Waveform relaxation method

WRM allows to model a multi-physics system of which components have heterogeneous time constants. The system is split to model each component with respect to its own time constant. Then the communication between subsystems is done by an exchange of waveforms. A loop is performed, with a relaxation at each iteration, until convergence.

Let a Differential Algebraic Equation (DAE) represent a system on the time domain $T = [t_0, t_f]$:

$$\dot{y}(t) = h(y(t), z(t)), \tag{1}$$
$$0 = g\left(y(t), z(t)\right). \tag{2}$$

$$y : [t_0, t_f] \longmapsto \mathbf{R}^m,\ z : [t_0, t_f] \longmapsto \mathbf{R}^p,$$
$$f : (\mathbf{R}^m, \mathbf{R}^p) \longmapsto \mathbf{R}^m,\ g : (\mathbf{R}^m, \mathbf{R}^p) \longmapsto \mathbf{R}^p.$$

The system is decomposed into r subsystems. Each subsystem i satisfies:

$$\dot{y}_i(t) = h_i(y(t), z(t)), \tag{3}$$
$$0 = g_i(y(t), z(t)), \tag{4}$$

with

$$y(t) = [y_1(t), \ldots, y_{i-1}(t), y_i(t), y_{i+1}(t), \ldots, y_r(t)]^T,$$
$$z(t) = [z_1(t), \ldots, z_{i-1}(t), z_i(t), z_{i+1}(t), \ldots, z_r(t)]^T.$$

$$y_i : [t_0, t_f] \longmapsto \mathbf{R}^{m_i},\ z_i : [t_0, t_f] \longmapsto \mathbf{R}^{p_i},$$
$$f_i : (\mathbf{R}^{m_i}, \mathbf{R}^{p_i}) \longmapsto \mathbf{R}^{m_i},\ g_i : (\mathbf{R}^{m_i}, \mathbf{R}^{p_i}) \longmapsto \mathbf{R}^{p_i},$$
$$m = \sum_{i=1}^{r} m_i,\ p = \sum_{i=1}^{r} p_i.$$

Equation (3) is the differential equation of subsystem i, and (4) is the algebraic equation. In these equations, y are state variables and z coupling variables.

The WRM produces iteratively an approximation $(\tilde{y}^k(t), \tilde{z}^k(t))$ of the solution $(y(t), z(t))$, where k is the iteration index.

The initial iteration is fixed using the known values of y and z at time t_0. This is the extrapolation step:

$$\tilde{y}^0(t) = y(t_0),\ \tilde{z}^0(t) = z(t_0),\ \forall\ t \in\ [t_0, t_f]. \tag{5}$$

Then, at iteration k, the DAE (3)-(4) are solved successively from subsystem 1 to r using Gauss-Seidel relaxation process:

$$\dot{\tilde{y}}_i^k(t) = f_i(\tilde{Y}_i^k(t), \tilde{Z}_i^k(t)), \tag{6}$$

$$0 = g_i(\tilde{Y}_i^k(t), \tilde{Z}_i^k(t)), \tag{7}$$

with

$$\tilde{Y}_i^k(t) = [\tilde{y}_1^k(t), \ldots, \tilde{y}_{i-1}^k(t), \tilde{y}_i^k(t), \tilde{y}_{i+1}^{k-1}(t), \ldots, \tilde{y}_r^{k-1}(t)]^T,$$
$$\tilde{Z}_i^k(t) = [\tilde{z}_1^k(t), \ldots, \tilde{z}_{i-1}^k(t), \tilde{z}_i^k(t), \tilde{z}_{i+1}^{k-1}(t), \ldots, \tilde{z}_r^{k-1}(t)]^T.$$

The algorithm stops when the norm of the difference between two successive iterations is smaller than a given tolerance.

In the case of an exact resolution of (6)-(7), convergence of the WRM to the exact solution is proven [1], [3], [4]. In the case of numerical resolution, the convergence is always effective, but an error is introduced by the discretization schemes. Equations (6)-(7) are solved numerically by using the most adapted time-scheme to the subsystem i, so each subsystem is solved using its own time discretization. We choose to use a linear interpolation between two discrete values of a waveform to obtain the value of this waveform at any time of T.

III. Output space mapping

Computation time of an optimization process depends on the complexity of the model to be evaluated during the process. A precise model is often long to simulate, and conversely a fast model is less accurate. Space mapping techniques allow to perform a fast and precise optimization by using the advantages of both models.

The following optimization problem has to be solved:

$$x_f^\star = \arg\min_x f(x) \text{ such that } k_f(x) \leq \mathbf{0}, \tag{8}$$

with

$$f : \mathbf{X} \to \mathbf{R},\ k_f : \mathbf{X} \to \mathbf{R}^q,\ \mathbf{X} \subset \mathbf{R}^n.$$

Objective function f and constraints k_f form the fine model, with both high precision and computation time. A second model of the same problem is considered: c and k_c are the objective function and constraints of the coarse model, faster but less accurate. The coarse optimization problem associated is:

$$x_c^\star = \arg\min_x c(x) \text{ such that } k_c(x) \leq \mathbf{0}, \tag{9}$$

with

$$c : \mathbf{X} \to \mathbf{R},\ k_f : \mathbf{X} \to \mathbf{R}^q.$$

The principle of OSM is to optimize with the coarse problem, then to evaluate the fine model at the solution found to obtain correction of the coarse model. This process is applied iteratively. At the j-th iteration of the OSM procedure, we consider a corrector $O^j \in \mathbf{R}$ for the objective function and a corrector $\tilde{O}^j \in \mathbf{R}^q$ for the constraints. The corrected problem is:

$$x^j = \arg\min_x O^j.c(x) \text{ such that } \tilde{O}^j.k_c(x) \leq \mathbf{0}. \tag{10}$$

From the solution x^j, new correctors are computed by evaluating the fine model, so the number of evaluations of the fine model is equal to the number of iterations. The algorithm stops when a convergence criterion is satisfied: for example, when $\frac{\|x^j - x^{j-1}\|}{\|x^{j-1}\|}$ is less than a given tolerance ε. We can also use a criterion on the difference between fine and coarse models. The algorithm is given:

1. $j = 0$
2. Initial point x^0
3. $O^0 = \dfrac{f(x^0)}{c(x^0)}, \tilde{O}_i^0 = \dfrac{k_{f,i}(x^0)}{k_{c,i}(x^0)},\ i = 1, \ldots, q$
4. while $\dfrac{\|x^j - x^{j-1}\|}{\|x^{j-1}\|} > \varepsilon$
   - 4.1. $x^j = \arg\min_x O^j.c(x)$ s. t. $\tilde{O}^j.k_c(x) \leq \mathbf{0}$
   - 4.2. $O^{j+1} = \dfrac{f(x^j)}{c(x^j)},\ \tilde{O}_i^{j+1} = \dfrac{k_{f,i}(x^j)}{k_{c,i}(x^j)},\ i = 1, \ldots, q$
   - 4.3. $j = j + 1$

OSM implies choosing two models: one coarse and one fine. In a system of components with heterogeneous time constants, the WRM is an adapted way to obtain a fine model with a shorter computing time than a strongly coupled model.

IV. Application

The OSM strategy is applied to the optimization of a transformer. We consider a device composed of a circuit supplying a transformer (Fig. 1(a)): a pulse width modulation (PWM) voltage source, an LC filter, a resistor and a transformer. Two models of this device are necessary to apply the space mapping.

A. Coarse and fine models

The coarse model is a circuit model of the device (Fig. 1(b)), where the transformer is represented by an inductance $\mathcal{L} = \frac{\mu_0 \mu_r N^2 S}{\ell}$, with N the number of turns in the primary coil, S the section and ℓ the length of the magnetic core.

The fine model is a simulation by WRM where the system is decomposed into two subsystems (Fig. 1(c)): the circuit and the transformer. The circuit consists of the PWM voltage source with the LC filter and a current source. The transformer is modeled by 3D FEM (only one eighth of the transformer is modeled, Fig. 2) in vector potential formulation with a voltage coupling [9], [10]. The source of the circuit is the current i_R in the resistor, and the source of the transformer is the voltage v_c of the capacitor. In the WRM loop, at the k-th iteration, circuit part is solved with i_R^{k-1} as a source. Voltage v_c^k is obtained and used as source for the transformer. This gives i_R^k, and the loop goes to the next iteration. For FEM, the magnetic flux density $\boldsymbol{B}$ is expressed with respect to the vector potential $\boldsymbol{A}$:

$$\boldsymbol{B}(\boldsymbol{\chi},t) = \mathbf{curl}\boldsymbol{A}(\boldsymbol{\chi},t), \tag{11}$$

$$\boldsymbol{\chi} \in \mathcal{D} \subset \mathbf{R}^3, \quad t \in T.$$

By Ampere's law and the coupling equation we obtain the following system:

$$\mathbf{curl}\left(\frac{1}{\mu}\mathbf{curl}\boldsymbol{A}(\boldsymbol{\chi},t)\right) - \boldsymbol{N}(\boldsymbol{\chi})i_R(t) = 0, \tag{12}$$

$$\frac{\mathrm{d}}{\mathrm{d}t}\int_{\mathcal{D}} \boldsymbol{A}(\boldsymbol{\chi},t).\boldsymbol{N}(\boldsymbol{\chi})\mathrm{dv} + R.i_R(t) = v_c(t). \tag{13}$$

where $\boldsymbol{N} = \boldsymbol{J}/i_R$, with $\boldsymbol{J}$ the current density.

Last, time discretizations are different in the two subsystems. Because of the PWM, time-step for the first subsystem is $dt_1 = 5 \times 10^{-7}$ seconds, whereas in the transformer part, time-step is $dt_2 = 10^{-3}$ seconds.

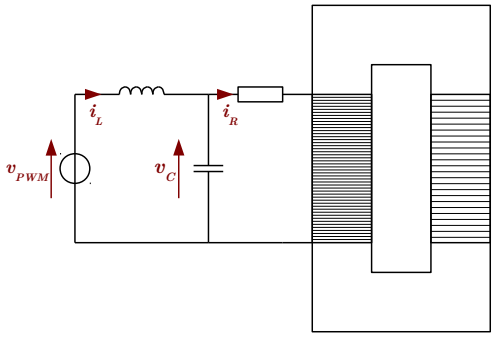

(a) Complete device.

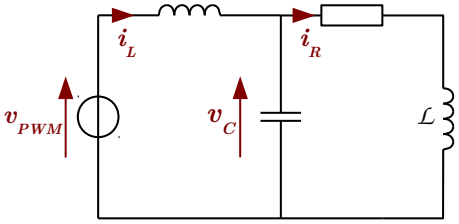

(b) Coarse model.

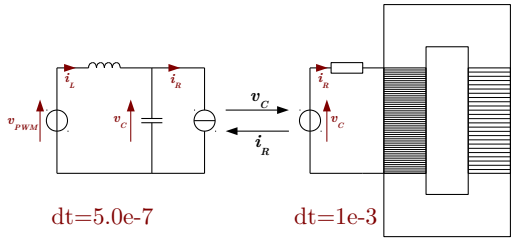

(c) Fine WRM model.

Fig. 1. The coarse and fine models of the device.

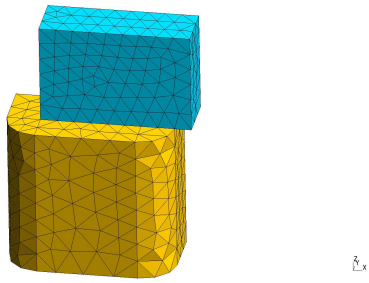

Fig. 2. Mesh of the eighth of transformer used for the FEM.

B. Optimization problem

The aim is to minimize the transformer mass m, and to impose RMS current value into the transformer. The design variables are width L and height H of the transformer: all other dimensions are deduced from this two length (Fig. 3). These two length form the optimization variables: $x = [H, L]$. We denote by i_c and i_f the RMS values of current i_R, obtained respectively with the coarse and the fine model. The optimization problem is:

$$\begin{cases} \min\limits_{H,L} m(H,L), \\ 20\text{cm} \leq H \leq 40\text{cm}, \\ 12\text{cm} \leq L \leq 24\text{cm}, \\ H - \frac{2L}{3} > 0, \\ i_f = 3\ A. \end{cases} \tag{14}$$

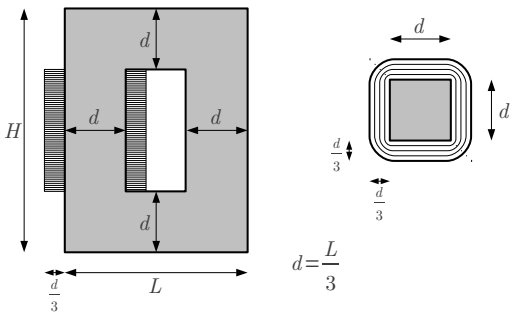

Fig. 3. Transformer's geometry.

OSM algorithm is applied to the optimization problem of the transformer. Objective function is the same for the two models, the correction is applied only on the constraint on the current in the primary coil. At iteration j of the OSM process, a corrector $\tilde{O}^j = \dfrac{i_f(x^j)}{i_c(x^j)}$ is applied to the value i_c such that the following corrected problem is solved:

$$\begin{cases} \min\limits_{H,L} m(H,L), \\ 20\text{cm} \leq H \leq 40\text{cm}, \\ 12\text{cm} \leq L \leq 24\text{cm}, \\ H - \frac{2L}{3} > 0, \\ \tilde{O}^j.i_c = 3\ A. \end{cases} \tag{15}$$

All the optimizations are executed with the corrected coarse model. The FEM is evaluated once per iteration to compute

TABLE I
SOLUTIONS AND OUPUTS OF THE OPTIMIZATION PROBLEM

	OSM	Reference (WRM)	Analytical
H	30.8478	30.8248	27.1054
L	12.0000	11.9971	11.9996
i_f	2.9996	3.0012	2.8051
m	19.7370	19.7113	16.9975
Number of f evaluations	3	90	-

the corrector. The algorithm stops when the difference between two iterations is small enough. Optimizations use sequential quadratic programming (SQP) algorithm. This algorithm needs an initial point to start with. For the first iteration, a random initial point is used. For the following iterations, the solution of the previous iteration is used. Five OSM procedures are performed, with five random initial points, and the best solution is kept. The algorithm used is the following:

1. random point x^0
2. while $\frac{\|x^j - x^{j-1}\|}{\|x^{j-1}\|} > \varepsilon$
   - 2.1. $\tilde{O}^j = \frac{i_f(x^{j-1})}{i_c(x^{j-1})}$
   - 2.2. $x^j = \arg\min_x m(x)$ s. t. $\tilde{O}^j . i_c(x) = 3$
   - 2.4. $j = j + 1$

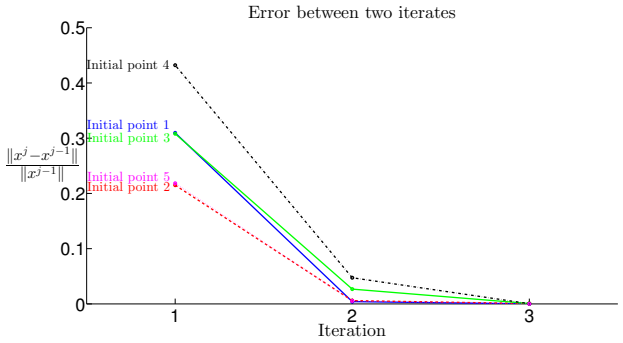

(a) Evolution of the error between two iterations vs space-mapping iterations.

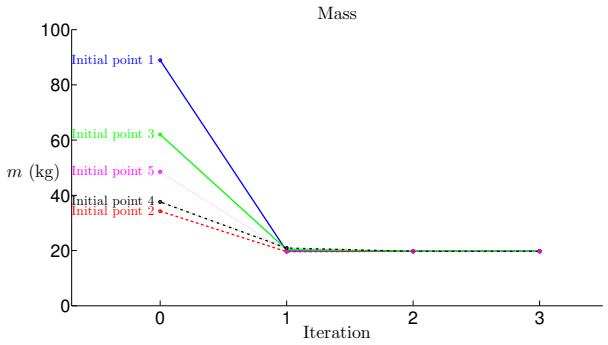

(b) Evolution of the transformer mass vs space-mapping iterations.

Fig. 4. Evolution of the error and of the mass vs space mapping iterations.

We compare in Table I the best solution obtained by using: 1. The OSM strategy. 2. An optimization with the WRM model. 3. An optimization with the analytical model. Reference solution is the solution obtained by the optimization with the WRM model. The OSM process stops at iteration j when the criterion $\frac{\|x^j - x^{j-1}\|}{\|x^{j-1}\|}$ is inferior to a given tolerance ε. The OSM algorithm converges quickly to a solution which minimize the transformer mass: on the five trials, three iterations maximum are enough to obtain the optimum (Fig. 4(a)), so FEM is evaluated three times, and the objective function decreases at each iteration (Fig. 4(b)). The computation time of the optimization process is considerably reduced due to the few evaluations of the FEM, but the solution is close to the reference solution. Compared to the reference solution, the error on the objective function is 13.77% with the analytical model but 0.13% with OSM.

V. CONCLUSION

A multirate system is composed of components with very different time constants that are evaluated many times during the optimization process. In order to reduce optimization time, an OSM strategy is applied to solve the problem. Two models of the system are chosen: an analytical one and a FEM. FEM is computed using the WRM, which allows to simulate each subsystem with respect to its own time constant and guarantees the consistency of the result with a reasonable computation time. The joint action of OSM and WRM allows to obtain a solution as accurate as WRM but in a shorter time.

REFERENCES

[1] E. Lelarasmee, A. Ruehli, and A. Sangiovanni-Vincentelli, *The waveform relaxation method for time-domain analysis of large scale integrated circuits*, Computer-Aided Design of Integrated Circuits and Systems, IEEE Transactions on, vol. 1, no. 3, pp. 131 145, july 1982.

[2] S. Schöps, H. De Gersem, and A. Bartel, *A cosimulation framework for multirate time integration of field/circuit coupled problems*, Magnetics, IEEE Transactions on, vol. 46, no. 8, pp. 3233 3236, aug. 2010.

[3] M. Arnold and M. Gunther, *Preconditioned dynamic iteration for coupled differential-algebraic systems*, Bit Numerical Mathematics, vol. 41, no. 1, pp. 125, 2001.

[4] M. Crow, M. Ilic, and J. White, *Convergence properties of the waveform relaxation method as applied to electric power systems*, Circuits and Systems, IEEE International Symposium on, pp. 18631866 vol.3, may 1989.

[5] Z. Guofo, W. Qiya, and R. Wanbin, *An output space-mapping algorithm to optimize the dimensional parameter of electromagnetic relay*, Magnetics, IEEE Transactions on, vol. 47, no. 9, pp. 21942199, sept. 2011.

[6] J. Bandler, Q. Cheng, D. Gebre-Mariam, K. Madsen, F. Pedersen, and J. Sondergaard, *Em-based surrogate modeling and design exploiting implicit, frequency and output space mappings*, Microwave Symposium Digest, 2003 IEEE MTT-S International, vol. 2, june 2003, pp.1003 1006 vol.2.

[7] L. Encica, J. Paulides, E. Lomonova, and A. Vandenput, *Aggressive output space-mapping optimization for electromagnetic actuators*, Magnetics, IEEE Transactions on, vol. 44, no. 6, pp. 11061109, june 2008.

[8] T. Tran, F. Moussouni, S. Brisset, and P. Brochet, *Adapted output space-mapping technique for a bi-objective optimization*, Magnetics, IEEE Transactions on, vol. 46, no. 8, pp. 29902993, 2010.

[9] A. Bossavit, *A rationale for edge-elements in 3-d fields computations*, Magnetics, IEEE Transactions on, vol. 24, no. 1, pp. 7479, 1988.

[10] F. Piriou and A. Razek, *Finite element analysis in electromagnetic systems-accounting for electric circuits*, Magnetics, IEEE Transactions on, vol. 29, no. 2, pp. 16691675, 1993.